ISSN 0030-400X, Optics and Spectroscopy, 2017, Vol. 122, No. 1, pp. 147–154. © Pleiades Publishing, Ltd., 2017.
Original Russian Text © A.H. Gevorgyan, 2017, published in Optika i Spektroskopiya, 2017, Vol. 122, No. 1, pp. 161–168.

PHYSICAL OPTICS

Specific Features of the Circular Dichroism of a Chiral Photonic Crystal with a Defect Layer Inside in the Presence of a Gain

A. H. Gevorgyan*

Far Eastern Federal University, Russky Island, Vladivostok, 690950 Russia

**e-mail: agevorgyan@ysu.am*

Received February 29, 2016; in final form, August 8, 2016

Abstract—The specific features of the circular dichroism (CD) spectra of a cholesteric liquid crystal (CLC) layer with a defect layer inside in the presence of gain have been investigated. The features of the dependence of CD on the parameter characterizing the gain on the defect mode are analyzed for two cases: (i) gain is present in the defect layer and is absent in the CLC sublayers and (ii) gain is absent in the defect layer but is present in the CLC sublayers. It is shown that these dependences significantly differ in the two aforementioned cases. The dependences of the reflection, transmission, and absorption on the defect mode on the gain parameter have been investigated for incident light with both circular polarizations.

DOI: 10.1134/S0030400X17010088

INTRODUCTION

Researchers pay much attention to photonic crystals (PCs) in view of the progress of their application in photonics and other fields of science and technology. Chiral PCs, which possess additional polarization features, are of particular interest [1–4]. The best known representatives of chiral PCs are cholesteric liquid crystals (CLCs) and chiral smectics.

CLCs, along with the ability to self-organize their periodic photonic structure, have a large-scale easy deformability, high sensitivity, and highly flexible ability for modulating phase or morphology; for this reason, these structures with a photonic band gap (PBG) rapidly react to external effects and are widely used in various fields. Moreover, CLCs have unique optical properties: they possess only a first-order PBG (under normal incidence of light) for light with a circular polarization having the same direction of rotation as the chirality sign of the medium. The absorption and emission in CLCs also have polarization features. Beyond the PBG (but near its edges), anisotropic absorption (gain) causes anomalously strong (anomalously weak) absorption (emission).

Much attention is paid to lasing on edge modes in CLCs enriched with dyes in view of the prospects of designing compact, completely organic controlled mirrorless lasers with a wide potential for application: from miniature spectroscopic and medical devices to holographic laser displays [5–8]. In the general case, CLC lasers can be separated into three classes: (1) lasers working on edge modes, (2) lasers on defect modes, and (3) random lasers.

CLCs with an internal planar defect layer are of interest both directly from the aforementioned point of view and due to their potential applications as polarization narrow-band filters (mirrors), optical diodes, etc. Cholesteric LCs with defects of different types have been studied in the last decades to gain insight into the specific features of lasing on defect modes, characteristics of absorption/emission on these modes, etc. (see [9–23] and references therein).

In this paper, we report the results of studying the influence of gain on the circular dichroism (CD) of a CLC layer with a planar defect inside (Fig. 1) and the influence of gain on the reflection, transmission, and emission of the structure under consideration.

CD measurement is a spectral method; it allows one to study the structure and state of the molecules of a medium. Along with the rotation of the plane of polarization, optical activity also manifests itself in the CD (the ability of material to differently absorb right- and left-handed circularly polarized light). The characteristic form of the CD spectra recorded for protein or DNA molecules, which generally manifests itself in the UV range, reflects the chiral geometry of these molecules and is due to the superposition of circularly dichroic responses of randomly oriented molecules in a liquid solution [24]. The helical periodic structure of

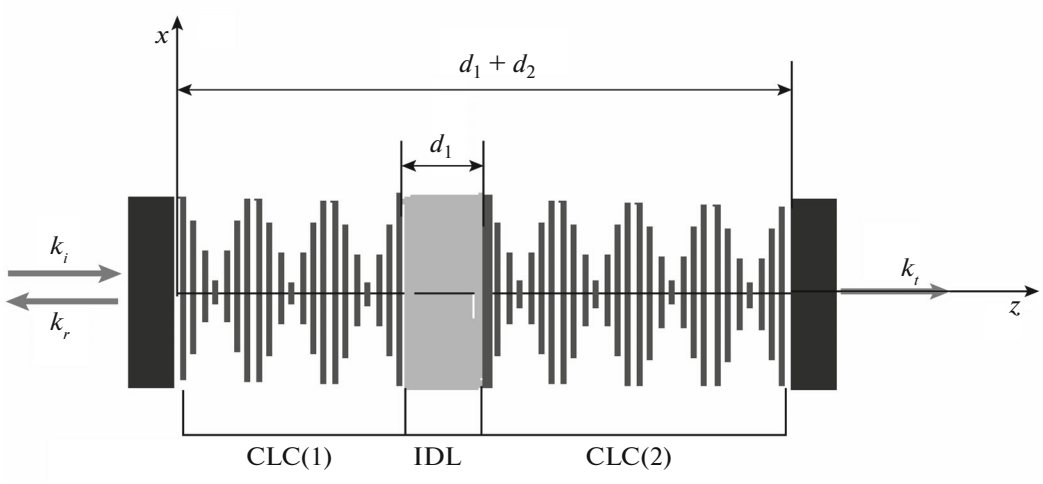

Fig. 1. Calculation model of CLC with an isotropic defect inside.

CLCs on the optical wavelength scale provides a strong and characteristic CD response in the visible range, i.e., the absorption of left- and right-handed circularly polarized waves in them is significantly different. The CD value can be defined as

$$\Delta A = A^l - A^r, \tag{1}$$

where $A = 1 - (R + T)$ characterizes the light energy absorbed in the system (R and T are, respectively, the energy reflectance and transmittance) and $A^{l,r}$ are the absorption coefficients for the system exposed to left- and right-handed circularly polarized light, respectively.

RESULTS AND DISCUSSION

Let us analyze the spectral properties of a CLC with an isotropic internal defect layer (Fig. 1). The transmission of a plane-polarized wave through this system will be analyzed by the modified Ambartsumyan method of adding layers [9].

We will decompose the electric field strengths of the incident, reflected, and transmitted waves into components oriented parallel (p polarization) and perpendicular (s polarization) to the plane of incidence:

$$\mathbf{E}_{i,r,t} = E^p_{i,r,t}\mathbf{n}_p + E^s_{i,r,t}\mathbf{n}_s = \begin{pmatrix} E^p_{i,r,t} \\ E^s_{i,r,t} \end{pmatrix}, \tag{2}$$

where the subscripts i, r, and t stand for the incident, reflected, and transmitted waves, respectively, and $\mathbf{n}_p$ and $\mathbf{n}_s$ are the unit vectors of p and s polarizations.

The solution to the problem can be written as

$$\begin{bmatrix} E^p_r \\ E^s_r \end{bmatrix} = \begin{bmatrix} R_{pp} & R_{ps} \\ R_{sp} & R_{ss} \end{bmatrix} \begin{bmatrix} E^p_i \\ E^s_i \end{bmatrix}, \quad \begin{bmatrix} E^p_t \\ E^s_t \end{bmatrix} = \begin{bmatrix} T_{pp} & T_{ps} \\ T_{sp} & T_{ss} \end{bmatrix} \begin{bmatrix} E^p_i \\ E^s_i \end{bmatrix}, \tag{3}$$

where $\hat{R}$ and $\hat{T}$ are the 2×2 reflection and transmission matrices of this system.

According to the method in use, if there is a system consisting of two adjacent (from left to right) layers A and B, the reflection and transmission matrices of the $A + B$ system (specifically, $\hat{R}_{A+B}$ and $\hat{T}_{A+B}$) are expressed in terms of the corresponding matrices of layers A and B using matrix equations:

$$\begin{aligned} \hat{R}_{A+B} &= \hat{R}_A + \tilde{\hat{T}}_A \hat{R}_B [\hat{I} - \tilde{\hat{R}}_A \hat{R}_B]^{-1} \hat{T}_A, \\ \hat{T}_{A+B} &= \hat{T}_B [\hat{I} - \tilde{\hat{R}}_A \hat{R}_B]^{-1} \hat{T}_A, \end{aligned} \tag{4}$$

where $\hat{I}$ is a unit matrix, and the tilde sign (a wavy line from above) denotes the reflection and transmission matrices for the backward light propagation direction. A CLC with an isotropic defect inside can be considered as a three-layer system, consisting of two CLCs layers (CLCs(1) and CLCs(2)), separated by an isotropic defect layer (IDL). The reflection and transmission matrices for this system are obtained in the following way: first, using formula (2), we match the isotropic layer with the CLC(2) layer from its left side; then, we match the first CLCs(1) layer to the obtained system, as previously, from the left side. Thus, the problem is reduced to the calculation of the reflection and transmission matrices for the outer CLC layers and the isotropic medium. The analytical solution to these problems is known [25, 26]. The thus constructed reflection and transmission matrices for the entire system make it possible to calculate the complex field amplitudes for the reflected and transmitted waves, while the reflectance, transmittance, rotation of the plane of polarization, polarization ellipticity,

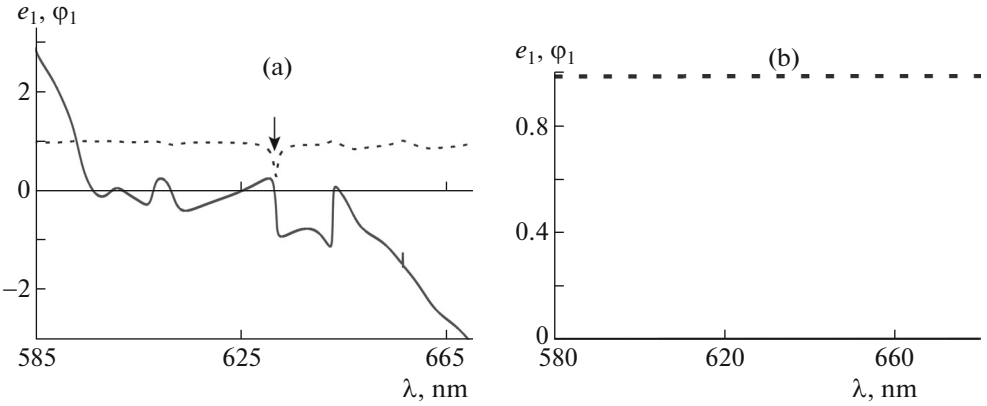

Fig. 2. Spectra of ellipticity e_1 (dotted lines) and azimuth φ_1 (solid lines) for the first EP: (a) $n = 1.8$ and $n_s = n_m$ and (b) $n = n_s = n_m$.

and other characteristics are expressed in terms of these amplitudes. In particular,

$$R = |E_R|^2/|E_i|^2, \quad T = |E_i|^2/|E_i|^2,$$
$$\psi = \arctan[2\mathrm{Re}(\chi)/(1 - |\chi|^2)]/2,$$
$$e = \arcsin[2\,\mathrm{Im}(\chi)/(1 + |\chi|)^2] / 2$$
$$(\chi = E_t^p/E_t^s),$$

etc.

Let us now pass to the eigen polarizations (EPs): two polarizations of the incident wave that do not change during the light transmission through the system. Having denoted the ratio of the complex components of field strength at the input of the system as χ_i ($\chi_i = E_i^p/E_i^s$) and the same ratio at the output of the system as χ_t ($\chi_t = E_t^p/E_t^s$), we derive from (2) a relationship between these ratios in the form

$$\chi_t = (T_{pp}\chi_i + T_{ps})/(T_{sp}\chi_i + T_{ss}). \quad (5)$$

Each optical system has two EPs, which are obtained by the replacement $\chi_i = \chi_t$ [[27]]. Hence, with allowance for (4), we arrive at the following expression for EPs χ_1 and χ_2:

$$\chi_{1,2} = \frac{T_{ss} - T_{pp} \pm \sqrt{(T_{ss} - T_{pp})^2 + 4T_{ps}T_{sp}}}{2T_{sp}}. \quad (6)$$

Ellipticities $e_{1,2}$ and azimuths $\psi_{1,2}$ of the EPs are expressed in terms of $\chi_{1,2}$ using the following formulas:

$$\psi_{1,2} = \arctan[2\mathrm{Re}(\chi_{1,2})/(1 - |\chi_{1,2}|^2)]/2,$$
$$e_{1,2} = \arcsin[2\,\mathrm{Im}(\chi_{1,2})/(1 + |\chi_{1,2}|^2)]/2. \quad (7)$$

Calculations were performed for a system with CLC layers having the following parameters: $n_o = \sqrt{\varepsilon_1} = 1.4639$ and $n_e = \sqrt{\varepsilon_2} = 1.5133$. These are ordinary and extraordinary refractive indices of CLC of the following composition: cholesteryl nonanoate : cholesteryl chloride : cholesteryl acetate = 20 : 15 : 6, which has a helix pitch lying in the optical range ($p = \pm 420$ nm) at room temperature (24°C) and exhibits diffraction reflection upon normal incidence of light in the wavelength range from 615 to 635 nm. The CLC helix is right-handed; hence, right-handed circularly polarized light incident on the defect-free CLC layer has a PBG, while left-handed circularly polarized light does not. Refractive index n of IDL was chosen to be $n = \sqrt{\varepsilon} = 1.7$. We assume that the n_o and n_e values for the CLC layers under consideration and n for the IDL are constant and frequency-independent and the imaginary parts are also frequency-independent; i.e., the optical dispersion effects are disregarded.

The presence of a thin defect in the CLC structure is known to induce a defect mode in the PBG. This mode manifests itself in the form of a dip in the reflection spectrum for right-handed circularly polarized light (diffracting circular polarization) and in the form of a peak in the reflection spectrum for left-handed circularly polarized light (nondiffracting circular polarization). The defect mode has either a donor or acceptor character, depending on the optical thickness of the defect layer: the defect-mode wavelength increases from the minimum to the maximum of the band gap with an increase in the defect optical thickness. Note that two defect modes arise near both band edges; then, with an increase in the defect-layer thickness, the long-wavelength mode is eliminated, while the short-wavelength mode is red-shifted [9].

The presence of a defect layer leads to a change in the EP; these changes are significant on the defect mode, being determined by the dependence of the reflectance on polarization on the defect layer edges. Specifically the dependence of the reflectance on polarization explains the occurrence of a peak in the reflection spectrum for left-handed circularly polarized light (nondiffracting circular polarization).

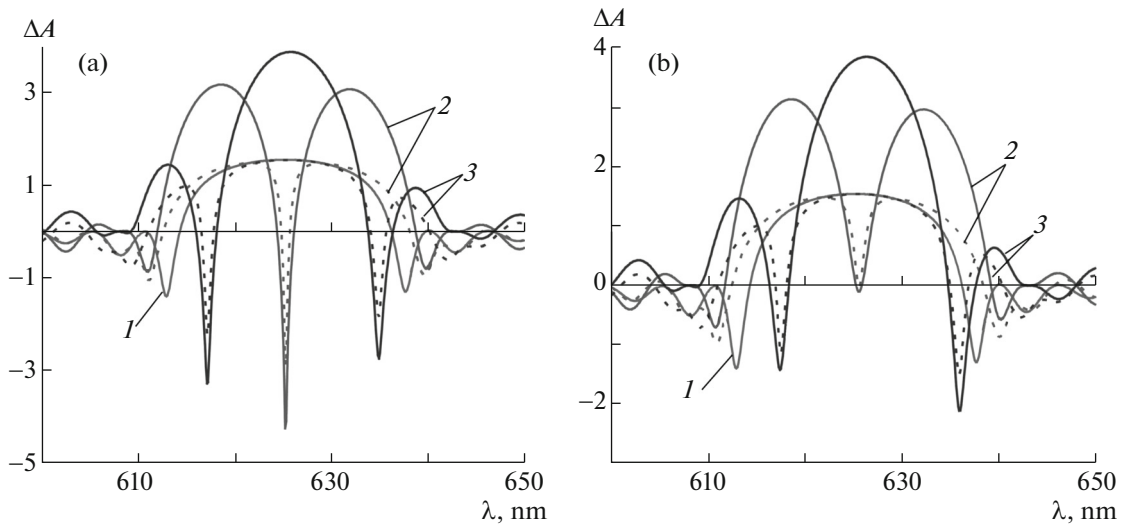

Fig. 3. CD spectra for (*1*) a homogeneous CLC layer and (*2*, *3*) a CLC layer with an IDL inside. (a) $n_s = n_m \neq n$, (b) $n_s = n_m = n$. Curve *2* corresponds to the case in which the defect-mode wavelength is at the center of the PBG ($d_1 = 2835$ nm and $\lambda_d = 625.26$ (a), $d_1 = 2000$ nm, and $\lambda_d = 625.455$ nm (b)), and curve *3* describes the case in which the defect-mode wavelength is near one of the PBG edges ($d_1 = 2950$ nm and $\lambda_d = 617.17$ nm (a), $d_1 = 2100$ nm and $\lambda_d = 617.5$ nm (b)).

One limiting case is of great interest. Specifically, this is the case in which refractive index n of the defect layer and coefficients n_s for the media adjacent to the system from both sides coincide with the average refractive index of the CLC layer, $n_m = \sqrt{\varepsilon_m} = \sqrt{\frac{(\varepsilon_1 + \varepsilon_2)}{2}}$, i.e., when $n = n_s = n_m$. Under these conditions, the EPs of the system coincide with both circular polarizations, i.e., coincide with the EP of the CLC layer, adjacent from both sides with the media having refractive indices coinciding with the average refractive index of the CLC layer.

Figure 2 shows the ellipticity and azimuth spectra of the first EP in the two above-mentioned cases: (a) the refractive index of the defect layer differs from the average refractive index of the CLC layer ($n_s = n_m \neq n$) and (b) these indices coincide ($n_s = n_m = n$). For the second EP, we have $e_2 = -e_1$, $\varphi_2 = -\varphi_1$. The defect mode is indicated by an arrow in Fig. 2a. When $n_s = n_m = n$, a peak does not arise in the reflection spectrum for left-handed circularly polarized light (nondiffracting circular polarization).

Let a CLC layer with an isotropic defect be enriched with dye molecules. In the presence of a pump wave, this system is amplifying; i.e., a planar cavity with an active element can be considered. The presence of dye molecules in the system leads to a change in its local refractive index. In this case, the effective imaginary parts of the effective local refractive indices of both CLC ($n''_{o,e}$) and isotropic defect (n'') are negative values ($n_{o,e} = n'_{o,e} + in''_{o,e}$ and $n = n' + in''$). In the presence of absorption, the imaginary parts $n''_{o,e}$ and n'' of the local refractive indices of the CLC and isotropic defect are positive.

The validity of applying these approaches was considered in greater detail in [28]. When the absorption of the system is nonzero, the light energy absorbed in it can be characterized by the value $A = 1 - (R + T)$. The specific features of CD in the presence of absorption were thoroughly analyzed in [29]. The A value in a gain medium is negative; in this case, CD will be characterized by the quantity

$$\Delta A = \ln(A^l) - \ln(A^r). \quad (8)$$

Figure 3 shows the CD spectra of a homogeneous CLC layer (curve *1*) and a CLC layer with an isotropic internal defect layer (curves *2* and *3*). Figures 3a and 3b correspond, respectively, to the cases in which the refractive index of the defect layer differs from the average refractive index of the CLC layer ($n_s = n_m \neq n$) and where these indices coincide ($n_s = n_m = n$). The solid curves describe the situation in which $n''_o = n''_e = 0$ and $n'' \neq 0$ ($\varepsilon'' = -0.0005$) (gain is present in the defect layer and is absent in the CLC sublayers). The dotted curves correspond to the case $n''_o = n''_e \neq 0$ ($\varepsilon''_1 = \varepsilon''_2 = -0.0005$) and $n'' = 0$ (gain is absent in the defect layer and is present in the CLC sublayers). Curves *2* and *3* describe the cases in which the defect-mode wavelength is, respectively, at the PBG center and near one of the PBG edges.

As can be seen in Fig. 3, the ΔA value in the PBG is positive for the homogeneous CLC layer; this is quite natural, because the CLC helix is right-handed, and

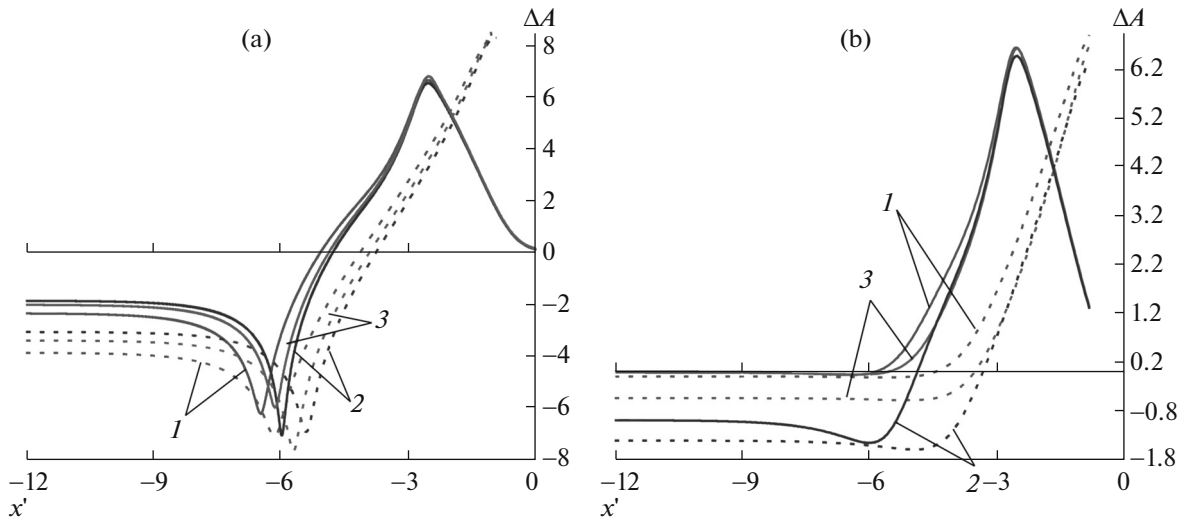

Fig. 4. Dependences of the CD value ΔA on parameter $x' = \ln(-\mathrm{Im}\,\varepsilon_m)$ (which characterizes the gain) at different defect-layer thicknesses, for (a) $n_s = n_m \neq n$ and (b) $n_s = n_m = n$. The solid curves correspond to the case $n_o'' = n_e'' = 0$ and $n'' \neq 0$, and the dotted curves describe the case $n_o'' = n_e'' \neq 0$ and $n'' = 0$. Curves *1–3* correspond, respectively, to the cases in which the defect-mode wavelength is at the center of the PBG ($d_1 = 2835$ nm and $\lambda_d = 625.26$ nm (a), $d_1 = 2000$ nm and $\lambda_d = 625.455$ nm (b)), near the short-wavelength PBG edge ($d_1 = 2950$ nm and $\lambda_d = 617.17$ nm (a), $d_1 = 2100$ nm and $\lambda_d = 617.5$ nm (b)), and near the long-wavelength PBG edge ($d_1 = 2900$ nm and $\lambda_d = 631.065$ nm (a) and $d_1 = 1900$ nm and $\lambda_d = 633.9$ nm (b)).

complete selective reflection of right-handed circularly polarized light and complete transmission of left-handed circularly polarized light occur in the PBG. Emission for right-handed circularly polarized light is suppressed in the PBG, by analogy with the suppression of absorption; therefore, $\ln(A^l) > \ln(A^r)$. The ΔA value changes sign on the defect and edge modes. These modes are also characterized by the absence of reflection for right-handed circularly polarized light. Due to the multiple reflections from the periodic structure for this polarization, the effective light path length greatly exceeds that for left-handed circularly polarized light. Hence, we have $\ln(A^l) < \ln(A^r)$ on these modes; correspondingly, ΔA changes sign on them.

Let us now analyze the influence of gain on the CD. Figure 4 shows a dependence of CD value ΔA on parameter $x' = \ln(-\mathrm{Im}\,\varepsilon_m)$ (which characterizes the gain) at different defect layer thicknesses. Figures 4a and 4b correspond, respectively, to the cases in which the refractive index of the defect layer differs from the average refractive index of the CLC layer ($n_s = n_m \neq n$) and where these indices coincide ($n_s = n_m = n$). The solid curves describe the situation in which $n_o'' = n_e'' = 0$ and $n'' \neq 0$, and the dotted curves correspond to the case in which $n_o'' = n_e'' \neq 0$ and $n'' = 0$.

As can be seen in Fig. 4, in the case $n_o'' = n_e'' \neq 0$ and $n'' = 0$, the CD value first decreases with an increase in parameter x', passes through a minimum, increases, passes through a maximum, and tends to zero with a further increase in x'. The situation is different when $n_o'' = n_e'' = 0$ and $n'' \neq 0$. In this case, the CD value first decreases with an increase in x', passes through a minimum, and then begins to increase. To gain a deeper insight into the nature of the presented CD regularities, we analyzed the dependences of the reflection, transmission, and absorption on the defect mode on parameter x' for incident light of both circular polarizations. Figure 5 shows these dependences for different defect layer thicknesses at $n_s = n_m = n$.

Note that, in the case of incident light with diffracting circular polarization, the reflectance and transmittance pass through a sharp peak with an increase in parameter x'. The corresponding x' value can be assumed to be close to the defect-mode lasing threshold (see more details in [30–32]).

Furthermore, the plots presented below show that the existence of gain generally worsens the coupling between the two CLC sublayers and weakens the light tunneling through the optical barrier (defect layer). This situation occurs also in the presence of absorption [29].

To complete the pattern, Fig. 6 shows the evolution of the CD spectra with an increase in parameter x'. Figures 6a and 6b correspond to the case $n_s = n_m \neq n$,

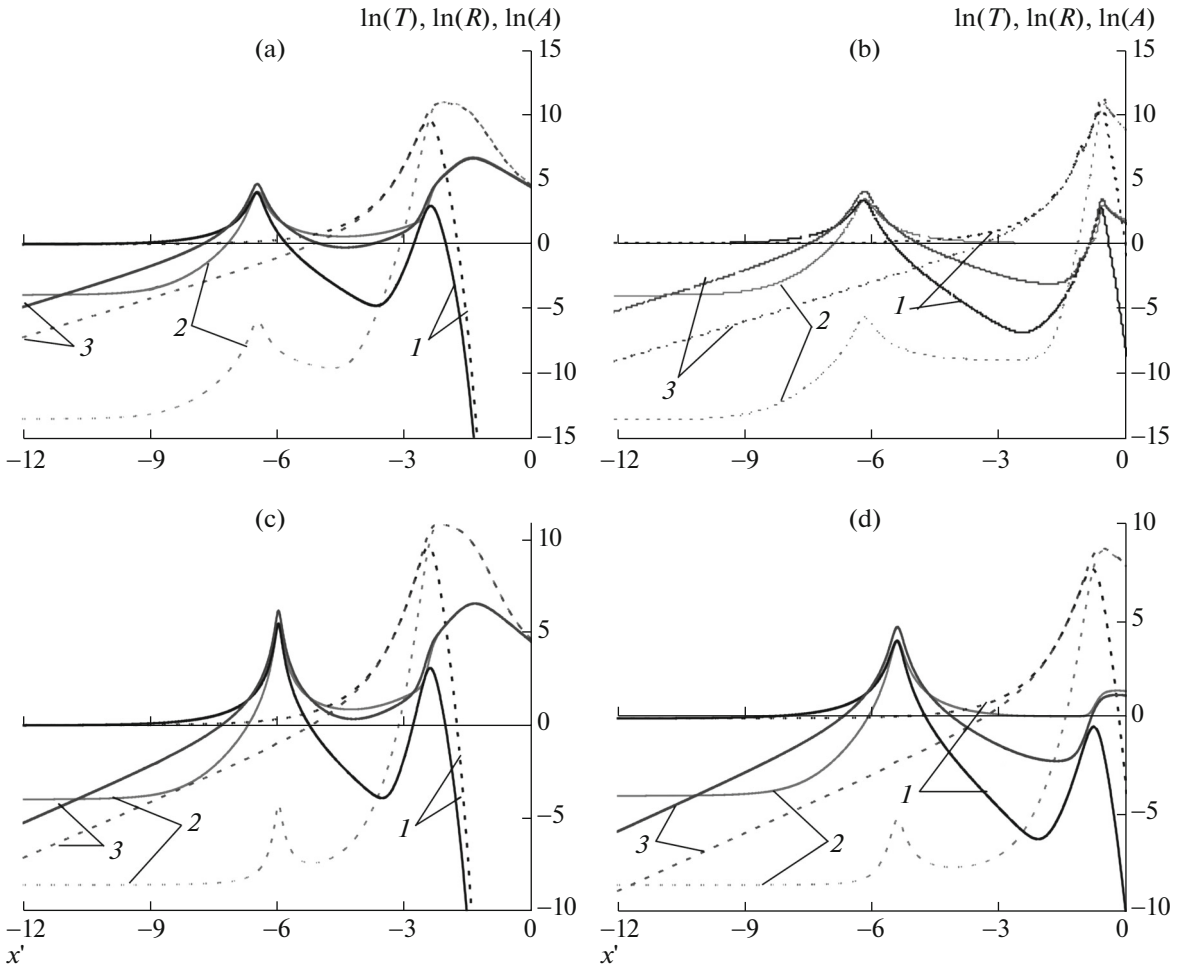

Fig. 5. Dependences of (*1*) ln(*T*), (*2*) ln(*R*), and (*3*) ln(*A*) on parameter $x' = \ln(-\mathrm{Im}\,\varepsilon_m)$, which characterizes gain at $n_s = n_m = n$: (a, c) $n_o'' = n_e'' \neq 0$, $n'' = 0$ and (b, d) $n_o'' = n_e'' = 0$, $n'' \neq 0$. The solid and dotted curves describe the cases in which the system is exposed to right- and left-handed circularly polarized light, respectively. (a, b) $d_1 = 2835$ nm, $\lambda_d = 625.26$ nm and (c, d) $d_1 = 2950$ nm, $\lambda_d = 617.17$ nm.

and Figs. 6c and 6d describe the case $n_s = n_m = n$. Furthermore, Figs. 6a and 6c correspond to the case $n_o'' = n_e'' \neq 0$ and $n'' = 0$, while Figs. 6b and 6d describe the case $n_o'' = n_e'' = 0$ and $n'' \neq 0$.

CONCLUSIONS

We have investigated the specific features of CD for a CLC layer with an isotropic defect in the presence of gain in the system. Two cases were analyzed: (i) the refractive index of the defect layer coincides with the average refractive index of CLC, and (ii) these indices are different.

The features of the CD spectra for a CLC layer with an internal defect layer in the presence of gain were studied. It was shown that the CD sign changes in the defect mode.

The specific features of the dependences of CD on the parameter characterizing the gain on the defect mode were analyzed for two cases: (i) gain is present in the defect layer and absent in the CLC sublayers and (ii) gain is absent in the defect layer and present in the CLC sublayers. These dependences were shown to be significantly different in the two aforementioned situations. In the former case, the CD first decreases with an increase in parameter x', passes through a minimum, increases, passes through a maximum, and then tends to zero with a further increase in x'. In the latter case, the CD first decreases with an increase in x', passes through a minimum, and then begins to increase.

The results of this study are also of interest for biophotonics. As was noted above, DNA and protein molecules have a helical structure. Therefore, in the case of parallel packing of these molecules, the ana-

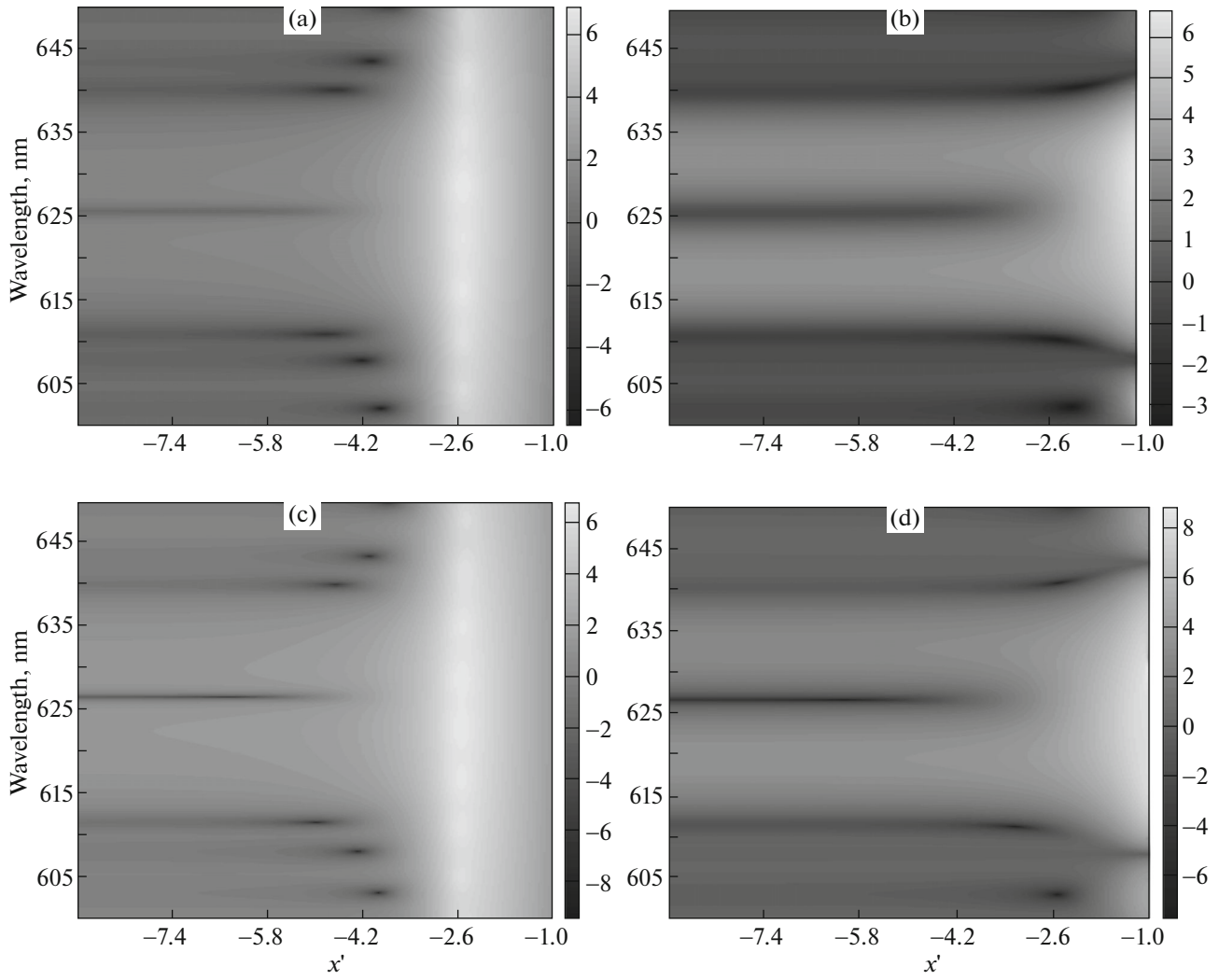

Fig. 6. Evolution of the CD spectra with an increase in parameter x': (a, b) $n_s = n_m \neq n$; (c, d) $n_s = n_m = n$; (a, c) $n_o'' = n_e'' \neq 0$, $n'' = 0$; and (b, d) $n_o'' = n_e'' = 0$, $n'' \neq 0$.

lyzed regularities for the aforementioned systems can also be observed in the X-ray range.

REFERENCES

1. P. G. de Gennes and J. Prost, *The Physics of Liquid Crystals* (Clarendon, Oxford, 1993).
2. V. A. Belyakov, *Diffraction Optics of Complex Structured Periodic Media* (Springer, New York, 1992).
3. M. Faryad and A. Lakhtakia, Adv. Opt. Photon. **6**, 225 (2014).
4. A. H. Gevorgyan, Phys. Rev. E **92**, 062501 (2015).
5. I. P. Ilchishin, E. A. Tikhonov, V. G. Tishchenko, and M. T. Spak, JETP Lett. **32**, 24 (1980).
6. V. I. Kopp, B. Fan, H. K. M. Vithana, and A. Z. Genack, Opt. Lett. **23**, 1707 (1998).
7. *Liquid Crystal Microlasers,* Ed. by L. M. Blinov and R. Bartolino (Transworld Research Network, Kerala, 2010).
8. H. Coles and S. Morris, Nat. Photon. **4**, 676 (2010).
9. A. H. Gevorgyan and M. Z. Harutyunyan, Phys. Rev. E **76**, 031701 (2007).
10. A. H. Gevorgyan, Opt. Commun. **281**, 5097 (2008).
11. A. H. Gevorgyan, A. Kocharian, and G. A. Vardanyan, Opt. Commun. **259**, 455 (2006).
12. Y.-C. Yang, Ch.-S. Kee, et al., Phys. Rev. E **60**, 6852 (1999).
13. J. Hodgkinson, Q. H. Wu, et al., Opt. Commun. **210**, 201 (2002).
14. J. Schmidtke, W. Stille, and H. Finkelmann, Phys. Rev. Lett. **90**, 083902 (2003).
15. V. I. Kopp and A. Z. Genack, Phys. Rev. Lett. **89**, 033901 (2002).
16. V. A. Belyakov and S. V. Semenov, J. Exp. Theor. Phys. **112**, 694 (2011).
17. S. Ya. Vetrov, M. V. Pyatnov, and I. V. Timofeev, Phys. Solid State **55**, 1697 (2013).

18. S. Ya. Vetrov, M. V. Pyatnov, and I. V. Timofeev, Phys. Rev. E **90**, 032505 (2014).
19. V. A. Belyakov and S. V. Semenov, J. Exp. Theor. Phys. **118**, 798 (2014).
20. V. A. Belyakov, Mol. Cryst. Liq. Cryst. **612**, 81 (2015).
21. Z. Muhammad, Q. A. Naqvi, and M. Faryad, Opt. Commun. **346**, 178 (2015).
22. A. H. Gevorgyan and K. B. Oganesyan, Laser Phys. Lett. **12**, 125805 (2015).
23. A. H. Gevorgyan, M. Z. Harutyunyan, et al., Laser Phys. Lett. **13**, 046002 (2016).
24. A. D. Rey, Soft Matter **6**, 3402 (2010).
25. A. H. Gevorgyan, Opt. Spectrosc. **92**, 207 (2002).
26. M. Born and E. Wolf, *Principles of Optics: Electromagnetic Theory of Propafation, Interference, and Diffraction of Light* (Pergamon, Oxford, 1964).
27. R. M. A. Azzam and N. M. Bashara, *Ellipsometry and Polarized Light* (North-Holland, Amsterdam, 1977).
28. A. V. Dorofeenko, A. A. Zyablovskii, A. A. Pukhov, A. A. Lisyanskii, and A. P. Vinogradov, Phys. Usp. **55**, 1080 (2012).
29. A. H. Gevorgyan, A. N. Kocharian, and G. A. Vardanyan, Liq. Cryst. **43**, 448 (2016).
30. V. A. Belyakov, Mol. Cryst. Liq. Cryst. **453**, 43 (2006).
31. V. A. Belyakov, Ferroelectrics **344**, 163 (2006).
32. A. H. Gevorgyan, K. B. Oganesyan, E. M. Harutyunyan, and S. O. Arutyunyan, Opt. Commun. **283**, 3707 (2010).

Translated by Yu. Sin'kov